10. DOSIMETRY OF INHALED PARTICLES IN THE RESPIRATORY TRACT

10.1 INTRODUCTION

Development of an efficient air-breathing respiratory tract was a critical requirement for mammalian evolution. The combination of airways and airspaces in an internalized and arborized arrangement that expands with incoming tidal air and contracts with its ebb led to the vertebrate lung. This very design that led to the close proximity of the alveolar air spaces to the outside environment for efficient air exchange also makes the lung vulnerable to insult by inorganic and organic dusts, and by microorganisms. The intense perfusion of these spaces by essentially the entire cardiac output also makes the lung vulnerable to many blood-borne, chemical, microbial, and immunologic agents.

It is a basic tenet of toxicology that the dose delivered to the target site, not the external exposure, is the proximal cause of a response. Therefore, there is increased emphasis on understanding the exposure-dose-response relationship. In the case of PM, exposure is what gets measured (or estimated) in the typical study and what gets regulated; inhaled dose is the causative factor. Even if inhaled dose could be easily defined, it fits within a complex continuum. For example, as illustrated in Figure 10-1, it is ultimately desirable to have a comprehensive biologically-based dose-response model that incorporates the mechanistic determinants of chemical disposition, toxicant-target interactions, and tissue response integrated into an overall model of pathogenesis. Mathematical dosimetry models that incorporate mechanistic determinants of disposition (deposition, absorption, distribution, metabolism, and elimination) of chemicals have been useful in describing relationships along this continuum (e.g., between exposure concentration and target tissue dose), particularly as applied to describing these relationships for the exposure-dose-response component of risk assessment. With each progressive level, incorporation and integration of mechanistic determinants allow further elucidation of the exposure-dose-response continuum and, depending on the knowledge of model parameters and fidelity to the biological system, a more accurate characterization of the pathogenetic process. Thus, once the site and

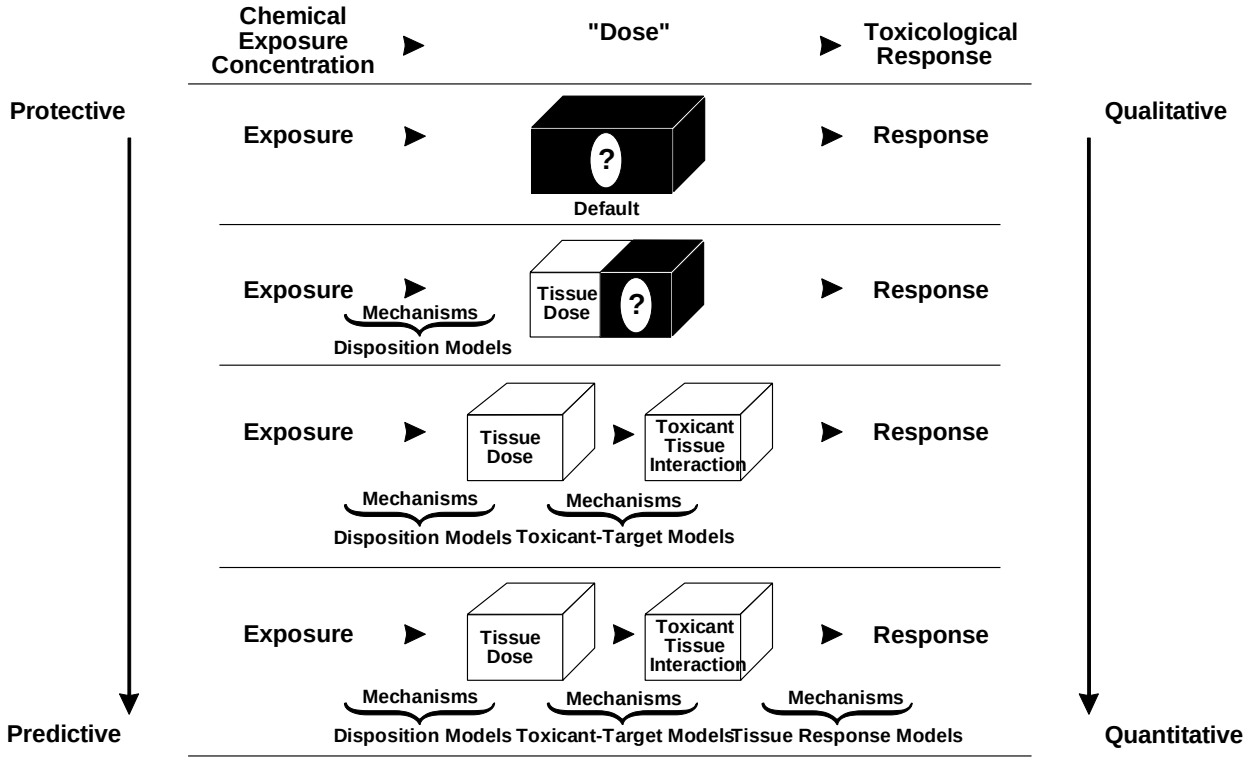

Figure 10-1. Schematic characterization of comprehensive exposure-dose-response continuum and the evolution of protective to predictive dose-response estimates.

Source: Adapted from Conolly (1990) and Andersen et al. (1992).

mechanisms are known, dosimetry may prove useful in linking exposure to internal dose and effects, and to the extrapolation of variability both within and across species. For example, a healthy individual and a person with emphysema will not get identical doses to specific lung regions even if their external exposure is identical. Knowledge of how and to what extent disease factors affect dose can assist in characterizing susceptible subpopulations. If a rat and a human are identically exposed, they will receive different doses to regions of the respiratory tract. Insofar as this is quantitatively understood, laboratory animal data can be made more useful in assessing human health risks.

Characterization of the exposure-dose-response continuum for PM requires the elucidation and understanding of the mechanistic determinants of inhaled particle dose, toxicant-target interactions, and tissue responses. Only the first level of characterization, i.e., description of the factors that influence inhaled dose has been accomplished to any degree for PM. Inhaled particles are deposited in the respiratory tract by mechanisms of interception, impaction, sedimentation, diffusion, and electrostatic precipitation. The relative contribution of each deposition mechanism to the fraction of inhaled particles deposited varies for each region of the respiratory tract (extrathoracic, ET; tracheobronchial, TB; and alveolar, A). Subsequent clearance of deposited particles depends on the initial deposition site, physicochemical properties of the particles (e.g., solubility), translocation mechanisms such as mucociliary transport and endocytosis by macrophages or epithelial cells, and on the time since initial deposition. Retained particle burdens and ultimate particle disposition are determined by the dynamic relationship between deposition and clearance mechanisms.

The biologically effective dose resulting from inhalation of airborne particles can be defined as the time integral of total inhaled particle mass, particle number, or particle surface area per unit of surface area (e.g., surface area of a given region such as the TB) or per unit mass of the respiratory tract. Choice of the metric to characterize the biologically effective inhaled dose should be motivated by insight on the mechanisms of action of the compound (or particles) in question. Conceptually, as illustrated in Figure 10-2, the exposure-dose-response continuum can be represented as events in the progression from exposure to disease. The components depicted in Figure 10-2 are not necessarily discrete, nor the only events in the continuum, and represent a conceptual temporal sequence. The left-most component of the continuum generally precedes any component to the right, but some impacts may be detectable in parallel. As our understanding of the continuum is supplemented by identification of the important intervening relationships and the components are characterized more precisely or with greater detail, the health events of concern can be viewed as a series of changes from homeostatic adaption, through dysfunction, to disease and death. The critical effect could become that biologic marker deemed most pathognomonic or of prognostic significance, based on validated hypotheses of the role of the marker in the development of disease. The appropriate dose metric would then be defined by a measure

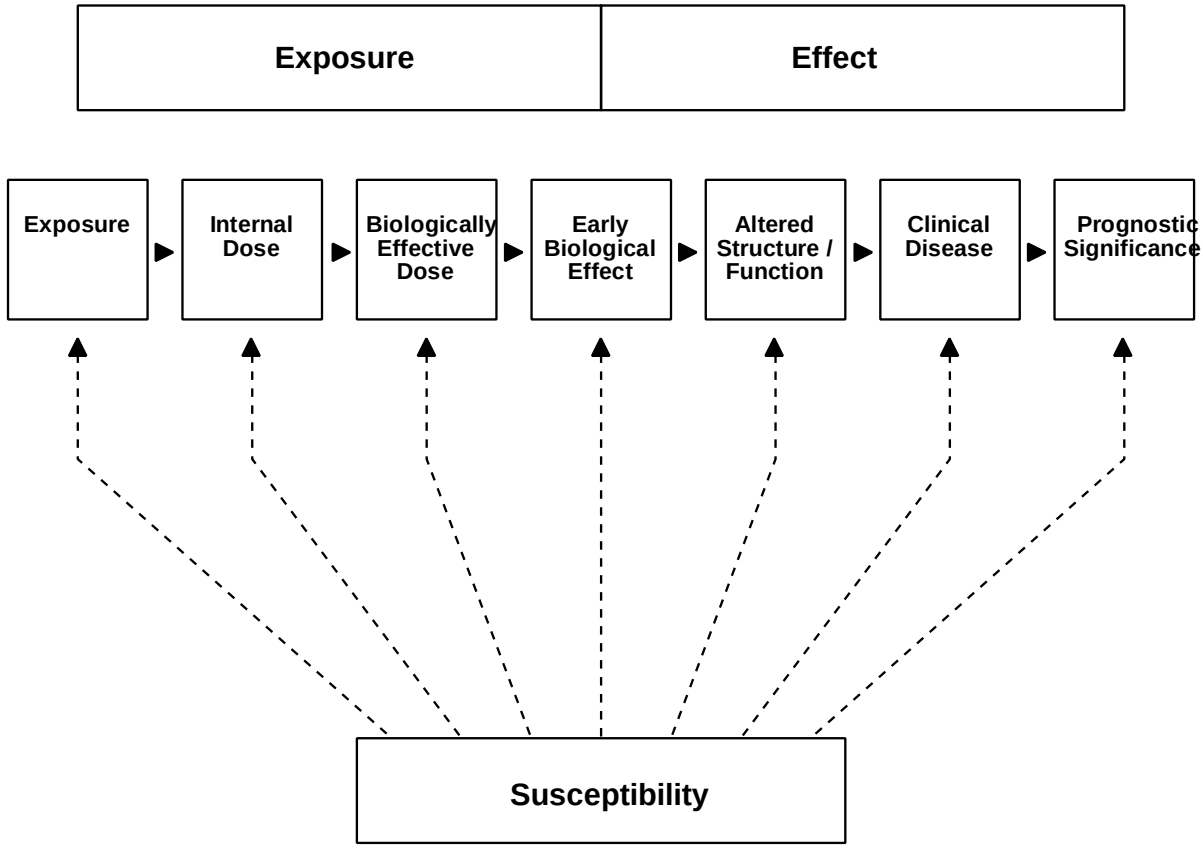

Figure 10-2. Biological marker components in sequential progression between exposure and disease.

Source: Schulte (1989).

that characterizes the biologically effective dose for the mechanism of action causing that critical effect.

Elucidation of the toxic moiety as well as the mechanism of action for PM have remained elusive, however. The link to the epidemiological findings discussed in Chapter 12 lies in understanding the sites of injury and the types of injury. The appropriate dose metric for PM might accurately be described by particle deposition alone of the particles exert their primary action on the surface contacted (Dahl et al., 1991). For longer-term effects, the deposited dose may not be a decisive metric, since particles clear at varying rates from the different respiratory tract regions. At this point, when considering the epidemiologic data, dose metrics can only be separated into two major categories: (1) the pattern and quantity of deposited particle burdens,

and (2) the pattern and quantity of retained particle burdens. The deposited dose or initial acute deposition (e.g., particle mass burden per 24-hours) may be relevant to "acute" effects observed in the epidemiologic studies such as "acute" mortality, hospital admissions, work loss days, etc. On the other hand, retained dose may be more appropriate for chronic responses such as induction of chronic disease, shortening of life-span ("premature mortality"), morbidity, or diminished quality of life.

Another aspect of the definition of the dose metric that would benefit from mechanism of action information include whether mass is the appropriate measure of particle burden and how to normalize the inhaled particle burdens. To date, most of the epidemiologic studies have relied upon the particle mass concentration ($\mu g/m^3$) to characterize particle exposures. Alternative expressions that may be more relevant to certain mechanisms of injury include numbers of particles or aggregate particle surface area. For example, the fine fraction contains by far the largest number of particles and those particles have a large aggregate surface area. Oberdörster et al. (1992) have shown ultrafine particles are less effectively phagocytosed by macrophages than larger particles. Anderson et al. (1990) have shown that the deposition of ultrafine particles in patients with COPD is greater than in healthy subjects. The need to consider particle number is accentuated when the high deposition efficiency of small particle numbers in the lower respiratory tract, the putative target for both the mortality and morbidity effects of PM exposures, is taken into account.

Insight on how PM causes injury would also inform what normalizing factor to use to define the dose metric. Particle mass or number burdens could be normalized to respiratory tract surface area, to lung mass, or to other anatomical or functional units critical to determining the toxicity such as ventilatory units, alveoli, or macrophages. Clearly, inhaled dose is important, but the most appropriate dose metric or metrics to quantitatively link with the observed acute or chronic health outcomes await elucidation of the pertinent mechanisms of injury and tissue response.

For the present document, average daily deposited particle mass burden in each region of the respiratory tract has been selected as the dose metric to characterize "acute" effects. Average retained particle mass burden in each region for humans and in the lower respiratory tract for laboratory animals has been selected as the dose metric for "chronic" effects. As discussed in Section 10.7.3., these choices were dictated by the selection of the dosimetry models and the

availability of anatomical and morphometric information. Both deposited particle mass and number burdens in each respiratory tract region are estimated for human exposures. Retained particle burdens are normalized per gram of lung tissue.

The chapter first describes important particle characteristics and the basic mechanisms of particle deposition and clearance in the respiratory tract. The available mathematical dosimetry models for humans and laboratory animals are reviewed as a background to the application presented in Section 10.7. Dosimetry models are selected for human exposure simulations and to perform interspecies extrapolation of laboratory animal toxicity studies. The rationale for selection of the extrapolation models is provided. An attempt is made to ascertain whether dosimetry modeling can provide insight into the apparent discrepancies between the epidemiologic and laboratory animal data, to identify plausible dose metrics of relevance to the available health endpoints, and to identify modifying factors that may enhance susceptibility to inhaled particles. Simulations of variability due to key modifying factors (age, gender, disease status) are also attempted. This information should be useful to the interpretation of health effects data in Chapters 11 and 12.

The chapter deals exclusively and generically with aerosols (i.e., both airborne droplets and solid particles, including the hygroscopic, acidic variety). It briefly reviews selected studies that have been reported in the literature on particle deposition and retention since the publication of the 1982 Air Quality Criteria Documents on Particulate Matter and Sulfur Oxides and the 1989 Acid Aerosols Issue Paper (U.S. Environmental Protection Agency; 1982, 1989), but the focus is on newer information.

10.2 CHARACTERISTICS OF INHALED PARTICLES

Information about particle size distribution aids in the evaluation of the effective inhaled dose. Because the characteristics of inhaled particles interact with the other major factors controlling comparative inhaled dose, this section discusses aerosol attributes requiring characterization and provides general definitions.

An aerosol is a suspension of finely dispersed solids or liquids in air. It is intrinsically unstable, and hence, tends to deposit both continuously and inelastically onto exposed surfaces. From the perspective of health-related actions of aerosols, interest is limited to particles that can

at least penetrate into the nose or mouth and that deposit on respiratory tract surfaces. For humans, this constraint ordinarily eliminates very coarse particles, viz., greater than about 100 μm diameter. Particles between 1 µm and 20 µm diameter are commonly encountered in the work place and the ambient air. Still smaller, i.e., submicron diameter particles (less than 1 µm in diameter) are generally the most numerous in the environmental air, with the number concentration of particles tending to increase markedly for smaller particles. Even particles down to the nanometer (nm) size domain are found in the atmosphere and are of interest, although until recently, these "ultrafine" particles were of greater interest to atmospheric scientists than to biomedical scientists. Typically, "ultrafine" aerosols are produced by highly energetic reactions (e.g., high temperature sublimation and combustion, or by gas phase reactions involving atmospheric pollutants). Note that 10 nm = 100 Ångstroms = 0.01 μm or 1×10^{-6} cm diameter.

Because aerosols can consist of almost any material, descriptions of aerosols in simple geometric terms can be misleading unless important factors relating to size, shape, and density are considered. Aerosol constituents are usually described in terms of their chemical composition and geometric or aerodynamic sizes. Additionally, aerosol particles may be defined in terms of particle surface area. It is important to note that aerosols present in natural and work environments all have polydisperse size distributions. This means that the particles comprising the aerosols have a range of geometric size, aerodynamic size, and surface area and are more appropriately described in terms of size distribution parameters. Aerosol sampling devices can be used to collect bulk or size fractions of aerosols to allow defining the size distribution parameters. In this procedure, the amount of particles in defined size parameter groups (number, mass, or surface area) is divided by the total number, mass, or surface of all particles collected and divided also by the size interval for each group. Data from the sampling device are then expressed in terms of the fraction of particles per unit size interval. The next step is to use this information to define an appropriate particle size distribution.

The lognormal distribution has been widely used for describing size distributions of radioactive aerosols (Hatch and Choate, 1929; Raabe, 1971) and is also generally used as a function to describe other kinds of aerosols. For many aerosols, their size distribution may be described by a lognormal distribution, meaning that the distribution will resemble the bell-shaped Gaussian error curve, if the frequency distribution is based on the logarithms of the

particle size. The lognormal distribution is a skewed distribution characterized by the fact that the logarithms of particle diameter are normally distributed. In linear form, the logarithmic mean is the median of the distribution. The standard deviation, σ, of this logarithmic normal distribution is a logarithm, so that addition and subtraction of this logarithm to and from the logarithmic mean is equivalent to multiplying and dividing the median by the factor σ_g, with ln $\sigma_g = \sigma$. The factor σ_g is defined as the geometric standard deviation. When any aerosol distribution is "normalized", it acquires parameters and properties equivalent to those of the Gaussian distribution. Accordingly, the only two parameters needed to describe the log normal distribution are the median diameter and the geometric standard deviation, σ_g, (ratio of the log 84%/log 50% size cut or log 50%/log 16% size cut, where the 50% size cut is the median). For a distribution formed by counting particles, the median is called the count median diameter (CMD). While there may be occasions when the number of the particles is of the greatest interest, the distribution of mass in an aerosol according to particle size is of interest if particle mass determines the dose of interest. Derivation of the particle mass distribution is essentially a matter of converting a diameter distribution to a diameter-cubed distribution since the volume of a sphere with diameter d is $\pi d^3/6$ and mass is simply the product of particle volume and physical density.

The cumulative distribution of a lognormally distributed size distribution is conveniently evaluated using log-probability graph paper on which the cumulative distribution forms a straight line (Figure 10-3). This distribution can be used for all three lognormally distributed particle size parameters discussed above, which are related as indicated in Figure 10-3. The characteristic parameters of this distribution are the size and σ_g. The CMD is characterized by the fact that half of the particles in the size distribution are larger than the CMD and half of the particles are smaller. Multiplying and dividing the CMD by σ_g yields the particle size interval for the distribution that contains about 68% of the particles by number.

When particles are not spherical, equivalent diameters can be used in place of the physical diameters of particles. A calculated parameter, the projected area diameter (diameter of a circle having a cross sectional area equivalent to the particles in the distribution of interest) is often used as the equivalent diameter.

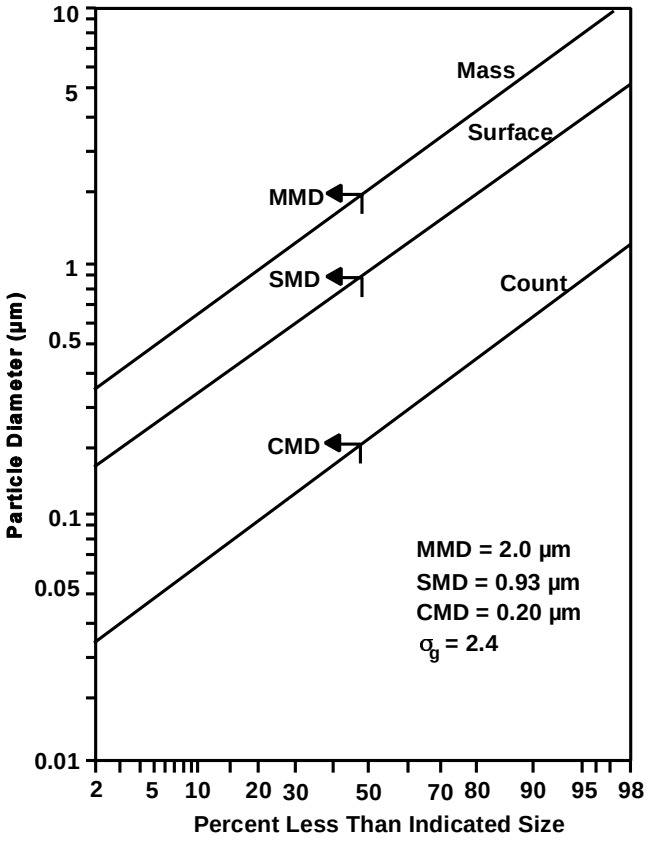

Figure 10-3. Lognormal particle size distribution for a hypothetical polydisperse aerosol.

The mass median diameter (MMD) and surface median diameter (SMD), also shown in Figure 10-3, are additional ways to describe size distributions of lognormally distributed aerosols. In these distributions, half of the mass or surface area of particles is associated with particles smaller than the MMD or SMD; the other half of the particles is associated with particles larger than the MMD or SMD, respectively.

The relationship of the various lognormal distribution parameters based on geometric diameter of particles is unique, since the CMD, SMD, and MMD are all lognormal with the same σ_g, but with different means that can be calculated. The CMD and σ_g can be determined and extrapolated to MMD, and SMD using the following relationships

$$\ln(\text{MMD}) = \ln(\text{CMD}) + 3(\ln\sigma_g)^2, \qquad (10\text{-}1)$$

and

$$\ln(SMD) = \ln(CMD) + 2(\ln\sigma_g)^2. \quad (10\text{-}2)$$

For most aerosols, it is useful to define a particle's size in terms of its aerodynamic size whereby particles of differing geometric size, shape and density are compared aerodynamically with the instability behavior of particles that are unit density (1 gm/cm^3) spheres. The aerodynamic behavior of unit density spherical particles can be determined, both experimentally and theoretically, consequently, the aerodynamic diameter constitutes a useful standard by which all particles can be compared in matters of inertial impaction and gravitational settling. Thus, if the terminal settling velocity of a unit density sphere of 10 μm diameter is measured in still air, the velocity induced by gravity would be ~3×10^{-1} cm/s. If the gravitational settling of an irregularly shaped particle of unknown density was measured and the same terminal velocity was obtained, the particle would have a 10 μm aerodynamic diameter (d_{ae}). Its tendency to deposit by inertial processes on environmental surfaces or onto the surfaces of the human respiratory tract will be the same as for the 10 μm unit density sphere.

A term that is frequently encountered is mass median aerodynamic diameter (MMAD), which refers to the mass median of the distribution of mass with respect to aerodynamic diameter. With commonly-encountered aerosols having low to moderate polydispersity, $\sigma_g \leq 2.5$, the Task Group on Lung Dynamics (TGLD) (1966) showed that mass deposition in the human respiratory tract could be approximated by the deposition behavior of the particle of median aerodynamic size in the mass distribution, the so-called MMAD. This is successful because the particles which dominate the mass distribution are those which deposit mainly by settling and inertial impaction.

In many urban environments, the aerosol frequency and mass distributions have been found to be bimodal or trimodal (Figure 10-4), usually indicating a composite of several log normal distributions where each aerosol mode was presumably derived from different formation mechanisms or emission sources (John et al., 1986). Conversely, in the laboratory, experimentalists often create aerosol distributions which are lognormal or normal, and very frequently, they generate monodisperse aerosols consisting of particles of nearly one size. The use of monodisperse aerosols of nearly uniform, unit density, spherical particles

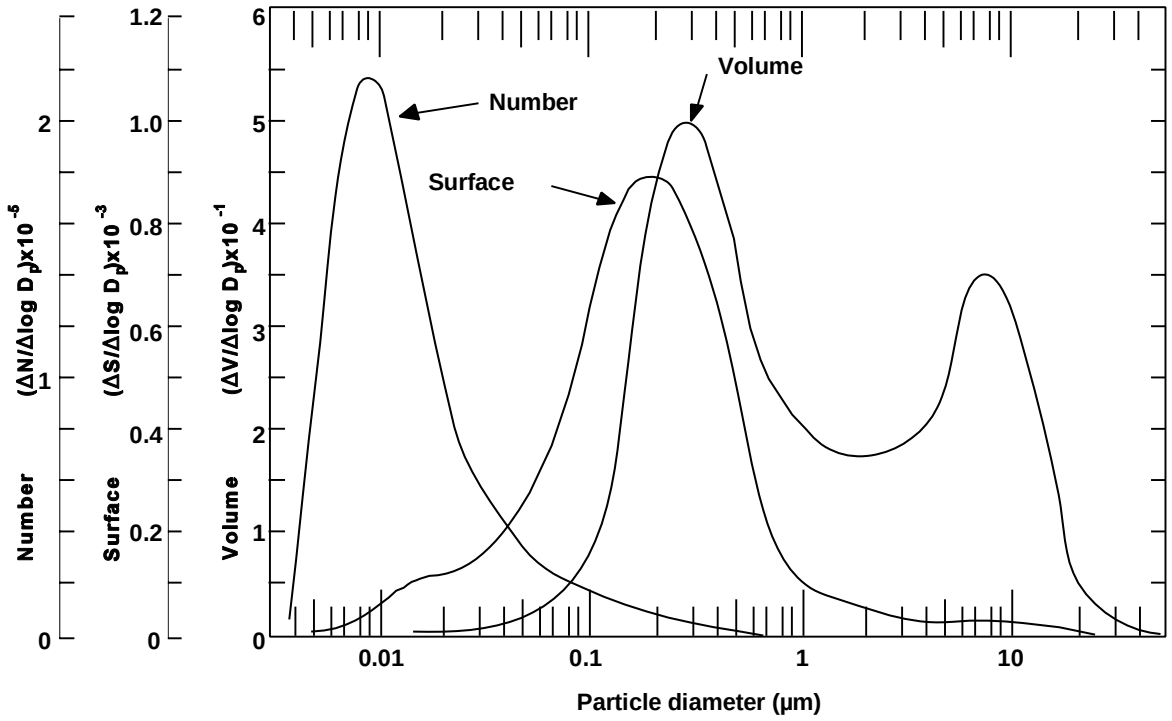

Figure 10-4. These normalized plots of number, surface, and volume (mass) distributions from Whitby (1975) show a bimodal mass distribution in a smog aerosol. Historically, such particle size plots were described as consisting of a coarse mode (2.5 to 15 μm), a fine mode (0.1 to 2.5 μm), and a nuclei mode (< 0.05μm). The nuclei mode would currently fall within the ultrafine particle range (0.005 to 0.1 μm).

greatly simplifies experimental deposition and retention measurements and also instrument calibrations. With nearly uniform particles, the mass, surface area and frequency distributions are nearly identical, another important simplification.

The terms count median aerodynamic diameter (CMAD) and surface median aerodynamic diameter (SMAD) might be encountered. These distributions are useful in that they include consideration of aerodynamic properties of the particles. If the particle aerodynamic or diffusive diameter is determined when sizing is done, then the median of the particle size distribution is the CMAD, or count median diffusive (or thermodynamic) diameter (CMDD or CMTD), respectively. If the mass of particles is of concern, then the median that is derived is the MMAD or mass median diffusive (or thermodynamic) diameter (MMDD or MMTD). Generally, MMTDs or MMADs are generally used to evaluate particle deposition patterns in the respiratory tract because deposition of inhaled aerosol particles, as discussed in detail later in this chapter, is

determined primarily by particle diffusive and aerodynamic properties of the particles rather than simply particle physical size, surface area, volume, or mass. Activity median aerodynamic diameter (AMAD) is the median of the distribution of radioactivity or toxicological or biological activity with respect to size. Both MMAD and AMAD are determined using aerosol sampling devices such as multistage impactors. When particles become smaller than about 0.1 μm diameter, their instability as an aerosol depends mainly on their interaction with air molecules. Like particles in Brownian motion, they are caused to "diffuse". For these small particles and especially for ultrafine particles, this interaction is independent of the particle density and varies only with geometric particle diameter. Very small particles are not expressed in aerodynamic equivalency, but instead to a thermodynamic-equivalent size. The thermodynamic particle diameter (d_{TH}) is the diameter of a spherical particle that has the same diffusion coefficient in air as the particle of interest. The activity median thermodynamic diameter (AMTD) is the diameter associated with 50 percent of the activity for particles classified thermodynamically.

The selection of the particle size distribution to associate with health effects depends on decisions about the importance of number of particles, mass of particles, or surface area of particles in producing the effects. In some situations, numbers of particles or mass of particles phagocytized by alveolar macrophages may be important; in other cases, especially for particles that contain toxic constituents, surface area may be the most important parameter that associates exposures with biological responses or pathology. These particle distributions should all be considered during the course of evaluating relationships between inhalation exposures to particles and effects resulting from the exposures.

Most of the discussion in the remainder of this chapter will focus on MMAD because it is the most commonly used measure of aerosol distributions. If MMAD is not measured directly, an alternative is to estimate MMAD from one of the particle size distributions that is based on physical size of the particles (CMD, MMD, and SMD), which can all be readily converted to MMAD. The approximate conversion of MMD to MMAD is made using the following relationship (neglecting correction for slip)

$$\text{MMAD} = \text{MMD} \cdot (\text{particle density})^{0.5}. \qquad (10\text{-}3)$$

By definition, MMDD = CMTD, because behavior of particles in this size category does not usually depend on aerodynamic properties.

Because small particles have a large aggregate surface area, aerosols comprised of such particles have increased potential for reactivity. For example, tantalum is a very stable, unreactive metal, whereas aerosols of tantalum particles can be caused to explode by a spark. The rates of oxidation and solubility are proportional to surface area as are the processes of gas adsorption and desorption, and vapor condensation and evaporation. Accordingly, special concerns arise from gas-particle mixtures and from "coated" particles. For a general review of atmospheric aerosols, their characteristics and behavior, the publication *Airborne Particles* prepared under the aegis of the National Research Council (1979) is recommended.

10.3 ANATOMY AND PHYSIOLOGY OF THE RESPIRATORY TRACT

The respiratory systems of humans and various laboratory animals differ in anatomy and physiology in many quantitative and qualitative ways. These differences affect air flow patterns in the respiratory tract, and in turn, the deposition of an inhaled aerosol. Particle deposition connotes the removal of particles from their airborne state due to their inherent instabilities in air as well as to addtional instabilities in air induced when additional external forces are applied. For example, in tranquil air, a 10 μm diameter unit-density particle only undergoes sedimentation due to the force of gravity. If a 10 μm particle is transported in a fast moving air stream, it acquires an inertial force that can cause it to deposit on a surface projecting into the air stream without significant regard to gravitational settling. For health-related issues, interest in particle deposition is limited to that which occurs in the respiratory tract of humans and laboratory animals during the respiration of dust-laden air.

Once particles have deposited onto the surfaces of the respiratory tract, some will undergo transformation, others will not, but subsequently, all will be subjected either to absorptive or non-absorptive particulate removal processes, e.g., mucociliary transport, or a combination thereof. This will result in their removal from the respiratory tract surfaces. Following this, they will undergo further transport which will remove them, to a greater or less degree, from the respiratory tract. Such particulate matter is said to have undergone clearance. To the extent

particulate matter is not cleared, it is retained. The temporal persistence of uncleared (retained) particles within the structure of the respiratory tract is termed retention.

Thus, either the deposited or retained dose of inhaled particles in each region is governed by the exposure concentration, by the individual species anatomy (e.g., airway size and branching pattern, cell types) and physiology (e.g., breathing rate, and clearance mechanisms), and by the physicochemical properties (e.g., particle size, distribution, hygroscopicity, solubility) of the aerosol. The anatomic and physiologic factors are discussed in this section. The physicochemical properties of particles were discussed in Section 10.2. Deposition and clearance mechanisms will be discussed in Section 10.4.

The respiratory tract in both humans and various experimental mammals can be divided into three regions on the basis of structure, size, and function: the extrathoracic (ET) region or upper respiratory tract (URT) that extends from just posterior to the external nares to the larynx, i.e., just anterior to the trachea; the tracheobronchial region (TB) defined as the trachea to the terminal bronchioles where proximal mucociliary transport begins; and the alveolar (A) or pulmonary region including the respiratory bronchioles and alveolar sacs. The thoracic (TH) region is defined as the TB and A regions combined. The anatomic structures included in each of these respiratory tract regions are listed in Table 10-1, and Figure 10-5 provides a diagrammatic representation of these regions as described in the International Commision on Radiological Protection (ICRP) Human Respiratory Tract Model (ICRP66, 1994).

Figure 10-6 depicts how the architecture of the respiratory tract influences the airflow in each region and thereby the dominant deposition mechanisms. The 5 major mechanisms (gravitational settling, inertial impaction, Brownian diffusion, interception and electrostatic attraction) responsible for particle deposition are schematically portrayed in Figure 10-6 and will be discussed in detail in Section 10.4.1.

In humans, the nasal hairs, anterior nares, turbinates of the nose, and glottic aperture in the larynx are areas of especially high air velocities, abrupt directional changes, and turbulence, hence, the predominant deposition mechanism in the ET region for large particles is inertial impaction. In this process, changes in the inhaled airstream direction or magnitude of air velocity streamlines or eddy components are not followed by airborne particles because of their inertia. Large particles (>5 μm in humans) are more efficiently removed from the

TABLE 10-1. RESPIRATORY TRACT REGIONS

Region	Anatomic Structure	Other Terminology
Extrathoracic (ET)	Nose Mouth Nasopharynx Oropharynx Laryngopharynx Larynx	Head airways region Nasopharynx (NP) Upper respiratory tract (URT) Naso-Oro-Pharyngo-Laryngeal (NOPL)
Tracheobronchial (TB)	Trachea Bronchi Bronchioles (including terminal bronchioles)	Lower conducting airways
Alveolar (A)	Respiratory bronchioles Alveolar ducts Alveolar sacs Alveoli	Gas exchange region Pulmonary region

Adapted from: Phalen et al. (1988).

airstream in this region. The respiratory surfaces of the nasal turbinates are in very close proximity to and designed to warm and humidify the incoming air, consequently they can also function effectively as a diffusion deposition site for very small particles and an effective absorption site for water-soluble gases. The turbinates and nasal sinuses are lined with cilia which propel the overlying mucous layer posteriorly via the nasopharynx to the laryngeal region. Thus, the airways of the human head are major deposition sites for the largest inhalable particles (>10 μm aerodynamic diameter) as well as the smallest particles (<0.1 micrometers diameter). For the most part, the ET structures are lined with a squamous, non-ciliated mucous membrane. Collectively, the movement of upper airway mucus, whether transported by cilia or gravity, is mainly into the gastrointestinal (GI) tract.

As air is conducted into the airways of the head and neck during inspiration, it first passes through either the nasal passages or mouth. Whereas nasal breathing is normal with most people most of the time, the breathing mode usually depends upon the work load. Work loads which tend to treble or quadruple minute ventilation i.e., go from 10 L/m to

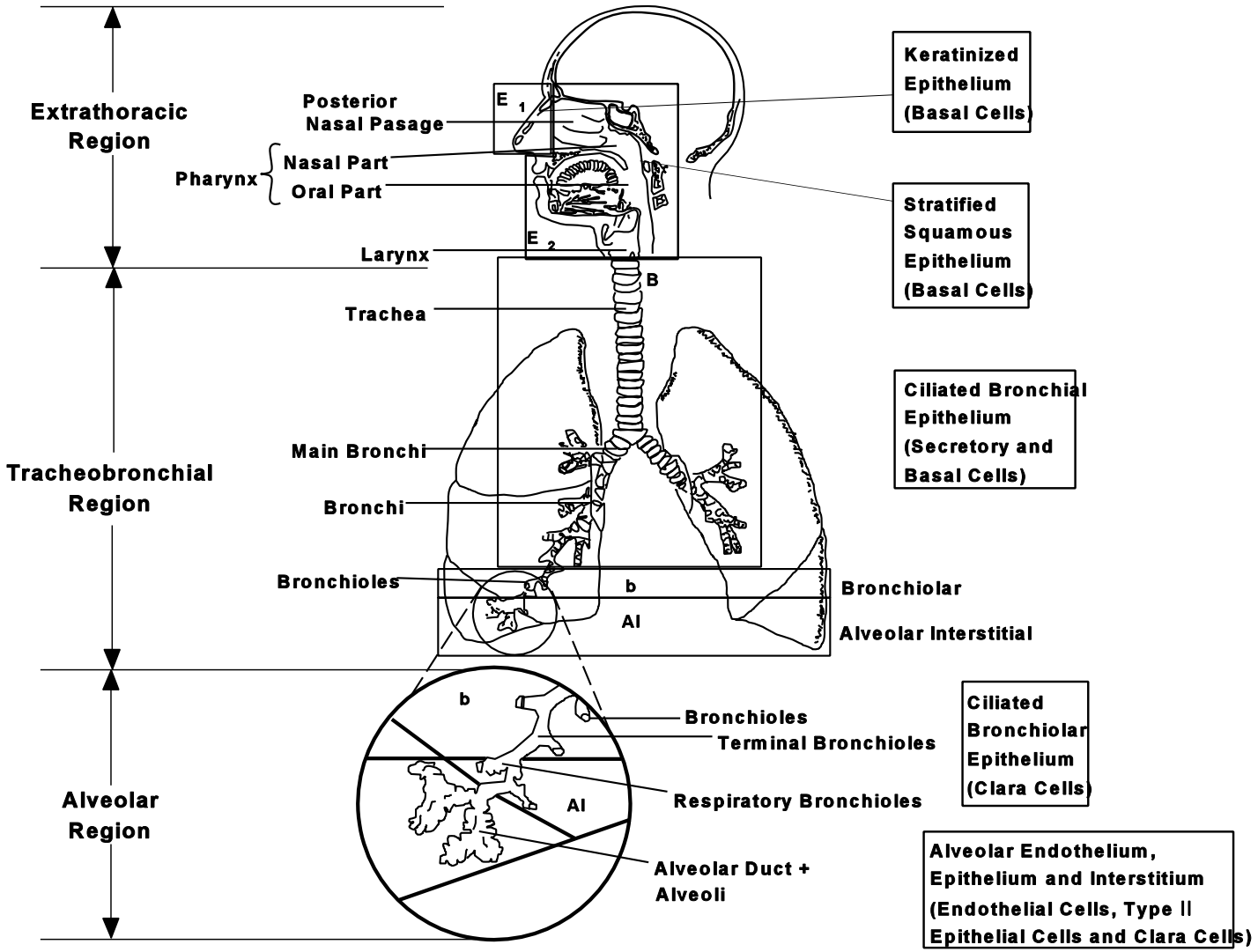

Figure 10-5. Diagrammatic representation of respiratory tract regions in humans.

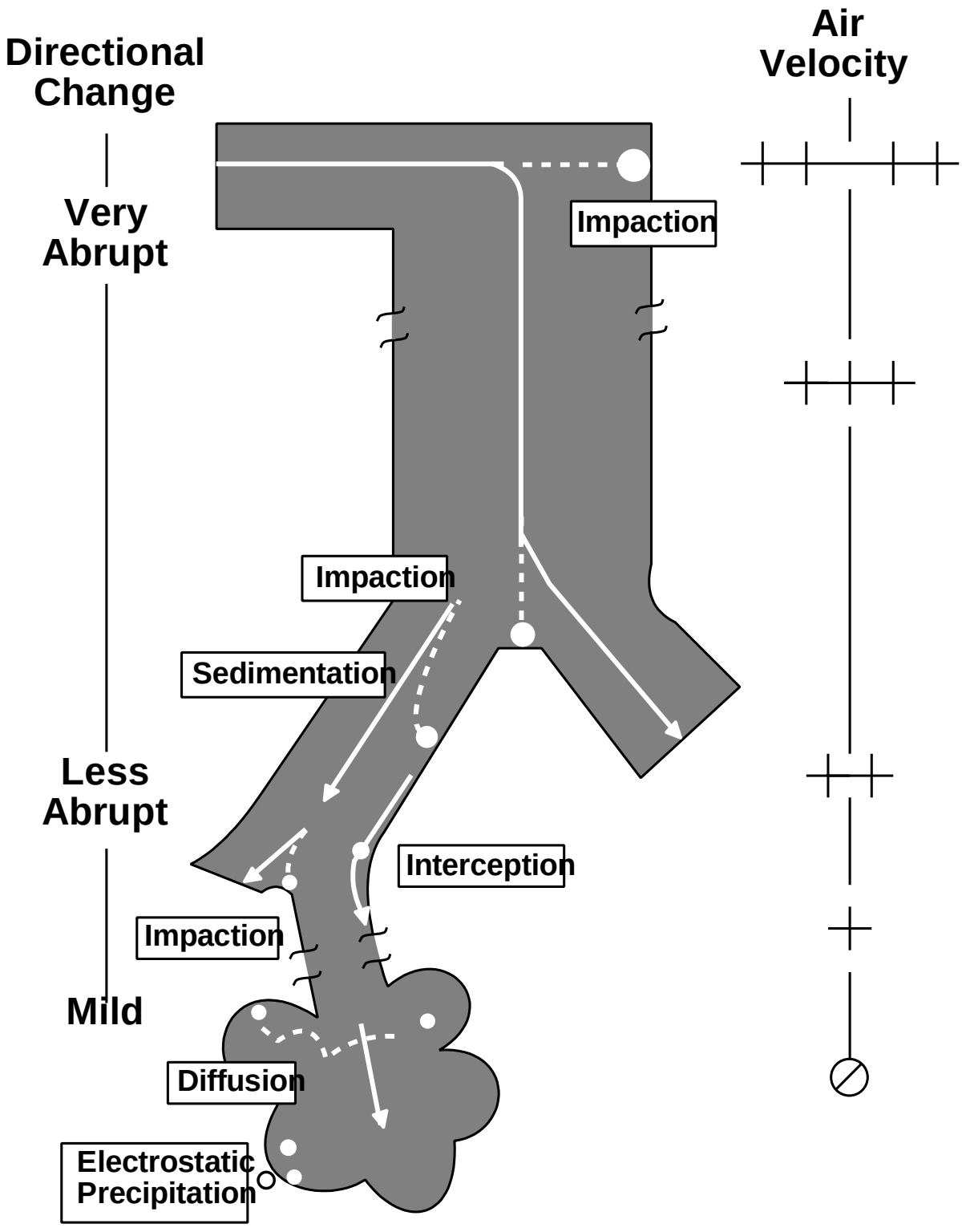

Figure 10-6. Schematic representation of five major mechanisms causing particle deposition where airflow is signified by the arrows and particle trajectories by the dashed line.

Source: Adapted from Casarett (1975); Raabe (1979); Lippmann and Schlesinger (1984).

30 to 40 L/m, cause most subjects to change from nasal to oronasal breathing. In either case, the inspired air then passes through the pharyngeal region into the larynx.

From the larynx, inspired air passes into the trachea, a cylindrical muscular- cartilaginous tube. The trachea measures approximately 1.8 cm diameter × 12 cm long in humans. The trachea, like other conducting airways of the lungs, is ciliated and richly endowed with secretory glands and mucus-producing goblet cells. The major or main stem bronchi are the first of approximately 16 generations of branching that occur in the human bronchial "tree". For modeling purposes, Weibel (1963;1980) described bronchial branching as regular and dichotomous, i.e., where the branching parent tube gives rise, symmetrically, to two smaller (by approximately $\sqrt[3]{2}$) tubes of the same diameter. While this pattern provides a simplification for modeling, the human bronchial tree actually has irregular dichotomous branching, wherein the parent bronchi gives rise to two smaller tubes of differing diameter and length. The number of generations of branching occurring before the inspired air reaches the first alveolated structures varies from about 8 to 18 (Raabe et al., 1976; Weibel, 1980). The junction of conducting and respiratory airways appears to be a key anatomic focus. Many inhaled particles of critical size are deposited in the respiratory bronchioles that lie just distal to this junction, and many of the changes characteristic of chronic respiratory disease involve respiratory bronchioles and alveolar ducts.

Impaction remains a significant deposition mechanism for particles larger than 2.5 μm aerodynamic equivalent diameter (d_{ae}) in the larger airways of the TB region in humans and competes with sedimentation, with each mechanism being influenced by mean flow rate and residence time, respectively. As the airways successively bifurcate, the total cross-sectional area increases. This increases airway volume in the region, and the air velocity is decreased. With decreases in velocity and more gradual changes in air flow direction as the branching continues, there is more time for gravitational forces (sedimentation) to deposit the particle. Sedimentation occurs because of the influence of the earth's gravity on airborne particles. Deposition by this mechanism can occur in all airways except those very few that are vertical. For particles ≈ 4 μm d_{ae}, a transition zone between the two mechanisms, from impaction to predominantly sedimentation, has been observed (U.S. Environmental Protection Agency, 1982). This transition zone shifts toward smaller particles for nose breathing.

The surface area of the adult human TB region is estimated to be about 200 cm^2 and its volume is about 150 to 180 mL. At the level of the terminal bronchiole, the most peripheral of the distal conducting airways, the mean airway diameter is about 0.3 to 0.4 mm and their number is estimated at about 6×10^4. As to the variability of bronchial airways of a given size, Weibel's model (1963) considered 0.2 cm diameter airways and noted that such airways occur from the 4th to 14th generations of branching, peaking in frequency around the 8th generation. An insight into the variabilities in various lung models was provided by Forrest (1993) who indicated that the number of terminal bronchioles incorporated in Weibel's model was about 66,000, whereas, Findeisen (1935) used 54,000 and Horsfield and Cumming (1968) estimated only 28,000. The transitional airways of the human lung, the respiratory bronchioles and alveolar ducts, undergo an average of another 6 generations of branching according to Weibel (1980) before they become alveolar sacs. On this basis, the dichotomous lung model indicates there should be about 8.4×10^6 branches (2^{23}), serving 3×10^8 alveoli. The "typical path" model of Yeh and Schum (1980), adopted by the National Council on Radiation Protection (NCRP) (Cuddihy et al., 1988), cites approximately 33,000 terminal bronchioles. The International Commission on Radiological Protection (ICRP) utilized the dimensions from three sources in its human respiratory tract model (ICRP66, 1994).

The parenchymal tissue of the lungs surrounds all of the distal conducting airways except the trachea and portions of the mainstem bronchi. This major branch point area is termed the mediastinum; it is where the lungs are suspended in the thorax by a band of pleura called the pulmonary ligament, the major blood vessels enter and leave the hilus of each lung, and the site of the mediastinal pleura which envelopes the heart and essentially subdivides the thoracic cavity.

Humans lungs are demarcated into 3 right lobes and 2 left lobes by the pleural lining. The suspension of the lungs in an upright human gives rise to a gradient of compliance increasing from apex to base and thereby controls the sequential filling and emptying of the lungs. Subdivisions of the lobes (segments) are not symmetrical due to a fusion of 2 (middle left lung) of the 10 lobar segments of the lung and occasionally an underdeveloped segment in the lower left lobe. Lobar segments can be related to specific segmental bronchi and are useful anatomical delineators for bronchoalveolar lavage.

The lung parenchyma is composed primarily of alveolated structures of the A region and the associated blood vessels and lymphatics. The parenchyma is organized into functional units called acini which consist of the dependent structures of the first order respiratory bronchioles. The alveoli are polyhedral, thin-walled structures numbering approximately 3×10^8 in the adult human lung. Schreider and Raabe (1981) provided a range of values, viz, 2×10^8 to 5.7×10^8. The parenchymal lung tissue can be likened to a thin sheet of pneumocytes (0.5 to 1.0 μm thickness) that envelopes the pulmonary capillary bed and is supported by a lattice of connective tissue fibers: these fibers enclose the alveolar ducts (entrance rings), support the alveolar septa, and anchor the parenchymal structures axially (e.g. from pulmonary veins) and peripherally (from the pleural surface).

The alveolar walls or septa are constructed of a network of meandering capillaries consisting mainly of endothelial cells, an overlying epithelium made of Type I cells or membranous pneumocytes (95% of the surface) with Type II cells or metabolically-active cuboidal pneumocytes (5% of the surface), and an interstitium or interseptal connective tissue space that contains interstitial histiocytes and fibroblasts (Stone et al., 1992). For about one-half of the alveolar surface, the Type I pneumocytes and the capillary endothelia share a fused basement membrane. Otherwise, there is an interstitial space within the septa which communicates along the capillaries to the connective tissue cuffs around the airways and blood vessels. The connective tissue spaces or basal lamina of these structures are served by pulmonary lymphatic vessels whose lymph drainage, mainly perivascular and peribronchial, is toward the hilar region where it is processed en route by islets of lymphoid tissue and filtered principally by the TB lymph nodes before being returned to the circulation via the subclavian veins. From the subpleural connective tissue, lymphatic vessels also arise whose drainage is along the lobar surfaces to the hilar region (Morrow, 1972).

The epithelial surface of the A region is covered with a complex lipo-proteinaceous liquid called pulmonary surfactant. This complex liquid contains a number of surface-active materials, primarily phospholipids, with a predominance of dipalmitoyl lecithin. The surfactant materials exist on the respiratory epithelium non-uniformly as a thin film (<0.01 μm thick) on a hypophase approximately 10 times thicker. This lining layer stabilizes alveoli of differing dimensions from collapsing spontaneously and helps to prevent the normal capillary effusate from diffusing from the interstitium into the alveolar spaces. The role of the lining layer as an environmental

interface is barely understood, especially in terms of how the layer may modify the physicochemical state of deposited particles and vice versa.

The epithelial surface of the A region, which can exceed 100 m^2 in humans, maintains a population of mobile phagocytic cells, the alveolar macrophage (AM), that have many important functions, e.g. removing cellular debris, eliminating bacteria and elaborating many cytologic factors. The AM is also considered to play a major role in non-viable particle clearance. The resident AM population varies, *inter alia*, according to conditions of particle intake, as does their state of activation. An estimate of the normal AM population in the lungs of non-smokers is about 7×10^9 (Crapo et al. 1982) while in the Fischer 344 rat, estimates are about 2.2×10^7 to 2.91×10^7 AM (Lehnert et al., 1985; Stone et al., 1992). According to prevailing views, the importance of AM-mediated particle clearance via the bronchial airways in the rat and human lungs may be different (refer to Section 10.4.2.).

The respiratory tract is a dynamic structure. During respiration, the caliber and length of the airways changes as do the angles of branching at each bifurcation. The structural changes that occur during inspiration and expiration differ. Since respiration, itself, is a constantly changing volumetric flow, the combined effect produces a complex pattern of airflows during the respiratory cycle within the conducting airways and volumetric variations within the A region. Even if the conducting airways were rigid structures and a constant airflow was passed through the diverging bronchial tree, the behavior of air flow within these structures would differ from that produced by the identical constant flow passed in the reverse or converging direction. Consequently, important distinctions exist between inspiratory and expiratory airflows through the airways, especially those associated with the glottic aperture and nasal turbinates. Distinctions occurring in particle deposition during inspiration and expiration are not as marked as those in airflow. This is because the particles with the greatest tendency to deposit, will deposit during inspiration and will mostly be absent from the expired air.

At rest, the amount of air that is inspired, the tidal volume (V_T), is normally about 500 mL. If a maximum inspiration is attempted, about 3300 mL of air can be added; this constitutes the inspiratory reserve volume (IRV). During breathing at rest, the average expired V_T is essentially unchanged from the average inspired V_T. At the end of a normal expiration, there still remains in the lungs about 2200 mL, the functional residual capacity (FRC). When a maximum expiration is made at the end of a normal tidal volume, approximately 1000 mL of additional air

will move out of the lung: this constitutes the expiratory reserve volume (ERV). Remaining in the lungs after a maximal expiration is the residual volume (RV) of approximately 1200 mL. These volumes and capacities are illustrated in Figure 10-7. From the perspective of air volumes within the respiratory tract, estimates are based on both anatomic and physiologic measurements. The ET airways have a volume in the average adult of about 80 mL, whereas the composite volume of the transitional airways is about 440 mL. At rest, the total volume in the lungs at end exhalation is usually around 2200 mL and is called the functional residual capacity (FRC). Both the RV and FRC tend to increase with age and in some forms of lung disease (e.g., COPD). The gas exchange volume of the lungs contacts with between 60 and 100 m^2 of alveolar epithelium depending on the state of lung inflation, viz, $Alv_{sa} = 22\ (V_L)^{2/3}$ where the surface area (Alv_{sa}) is in m^2 and the lung volume (V_L) in liters (or cubic decimeters). The alveolar volume is juxtaposed with a pulmonary capillary blood volume (70 to 230 mL) which varies with cardiac output and contacts an endothelial surface area of comparable size to that of the alveoli.

The average respiratory frequency of an adult human at rest is about 12 to 18 cycles per min. This indicates a cycle length of 4 to 5 s: about 40% for inspiration and 60% for expiration. With a 500 mL V_T, this results in a minute ventilation ($\dot{V}_E$) of about 6 to 7.5 L/min: about 60 to 70% of the $\dot{V}_E$ is considered alveolar ventilation due to the dead space volume constituting about 30 to 40% of the V_T. With the foregoing assumptions, the mean inspiratory and expiratory air flows will be about 250 mL/s and 166 mL/s, respectively. During moderate to heavy exercise, the $\dot{V}_E$ will increase by up to 10-fold or more (35 to 70 L/min or more). This is accomplished initially and primarily by an increase in V_T (V_T reaches approximately 2.0 L and frequency approximately 30 to 35 per min at a ventilation of 60 to 70 L per min). There is considerable variation in response. One impact of such an assumed change in $\dot{V}_E$ is that the duration of the respiratory phases become shorter and more similar, consequently, the mean inspired and expired air flows will both likely increase to about $\geq$2,000 mL/s. With nose breathing, an inspiratory airflow of

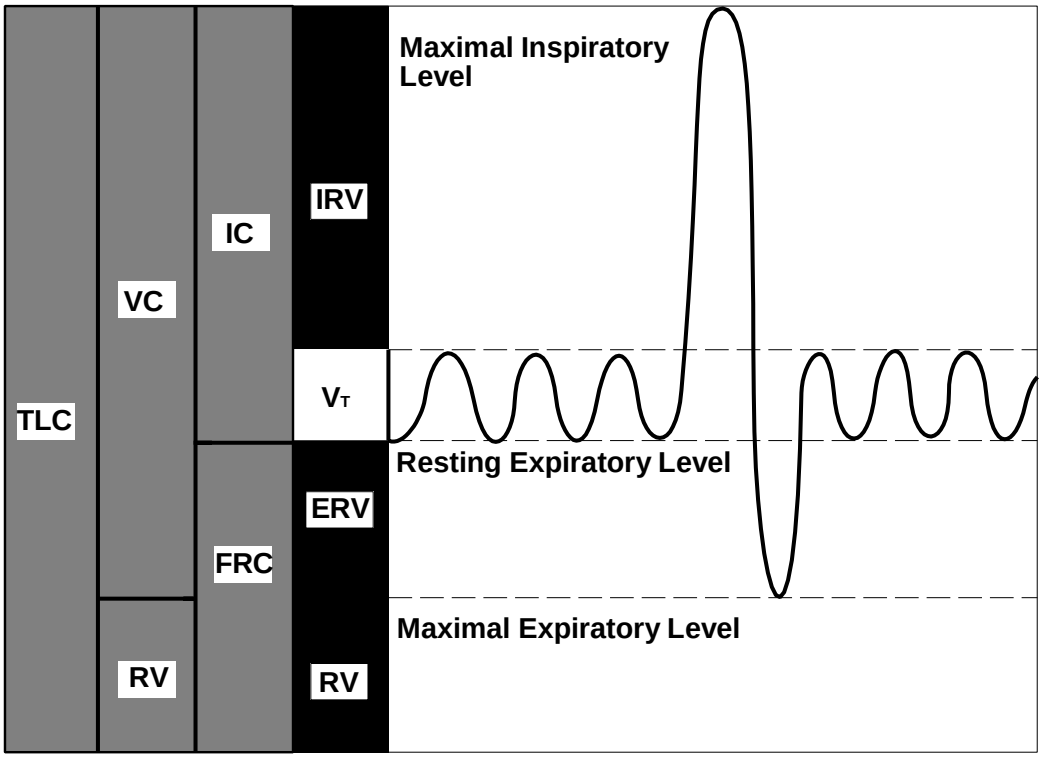

Figure 10-7. Lung volumes and capacities. Diagrammatic representation of various lung compartments, based on a typical spirogram. TLC, total lung capacity; VC, vital capacity; RV, residual volume; FRC, functional residual capacity; IC, inspiratory capacity; V_T, tidal volume; IRV, inspiratory reserve volume; ERV, expiratory reserve volume. Shaded areas indicate relationships between the subdivisions and relative sizes as compared to the TLC. The resting expiratory level should be noted, since it remains more stable than other identifiable points during repeated spirograms, hence is used as a starting point for FRC determinations, etc.

Source: Ruppel (1979).

800 mL/s would be expected to produce linear velocities in the anterior nares greater than 10 m/s.

Because of the irregular anatomic architecture of the nasal passages, the incoming air induces many eddies and turbulence in the ET airways. This is also true in the upper portions of the TB region largely due to the turbulence created by the glottic aperture. As the collective volume and cross sectional area of the bronchial airways increases, the mean airflow rates fall, but "parabolic airflow", a characteristic of laminar airflow does not develop because of the

renewed development of secondary flows due to the repetitive airway branching. Conditions of true laminar flow probably do not occur until the inspired air reaches the transitional airways. Whether air flow in a straight circular tube is laminar or turbulent is determined by a dimensionless parameter known as the Reynolds number (Re) which is defined by the ratio $\rho_a D_a U/\mu$ where ρ_a is the air density, D_a is the tube diameter, U is the air velocity, and μ is the viscosity of air. As a general rule, when Re is below 2000, the flow is expected to be laminar (Owen, 1969). See Table 10-2.

Pattle (1961) was the first investigator to demonstrate that the nasal deposition of particles was proportional to the product of the aerodynamic diameter (d_{ae}) squared and the mean inspiratory flow rate (Q); where the aerodynamic diameter is the diameter of a unit density sphere having the same terminal settling velocity (see Section 10.2) as the particle of concern. Albert et al. (1967) and Lippmann and Albert (1969) were among the earliest to report experimentally that the same general relationship governed inertial deposition of different uniformly-sized particles in the conducting airways of the TB region. Recent papers by Martonen et al. (1994a,b,c) have considered the influence of both the cartilaginous rings and the carinal ridges of the upper TB airways on the dynamics of airflow. As in the case of the glottic aperture, these structures appear to contribute to the non-uniformity of particulate deposition sites within these airways. Concomitantly, Martonen et al. have pointed to the limitations incurred by assuming smooth tubes in modeling the aerodynamics of the upper TB airways (see also Section 10.5.1.5).

Smaller particles, i.e. those with an aerodynamic size of between 0.1 and 0.5 μm, are the particles with the greatest airborne stability. They are too small to gravitate appreciably and are too large to diffuse; hence they tend to persist in the inspired air as a gas would, but in teams of alveolar mixing, they behave as "non-diffusible" gas. The study of these particles has provided very useful information on the distribution of tidal air under different physiologic conditions (Heyder et al., 1985). A recent analysis of airflow dynamics in human airways, conducted by Chang and Menon (1993), concluded that the measurement of flow dynamics aids in the understanding of particle transport and the development of enhanced areas of particle deposition.

Sedimentation becomes insignificant relative to diffusion as the particles become smaller. Deposition by diffusion results from the random (Brownian) motion of very small

TABLE 10-2. ARCHITECTURE OF THE HUMAN LUNG ACCORDING TO WEIBEL'S (1963) MODEL A, WITH REGULARIZED DICHOTOMY

Region	Generation	Number	Diameter (mm)	Length (mm)	Cum.[b] Length (mm)	Area[a] (cm^2)	Volume (mL)	Cum.[b] Volume (mL)	At flow of 1 L/sec: Speed (cm/s)	At flow of 1 L/sec: Reynolds Number
Trachea[c]	0	1	18	120.0	120	2.6	31	31	393	4,350
Main bronchus	1	2	12.2	47.6	167	2.3	11	42	427	3,210
Lobar bronchus	2	4	8.3	19.0	186	2.2	4	46	462	2,390
	3	8	5.6	7.6	194	2.0	2	47	507	1,720
Segmental bronchus	4	16	4.5	12.7	206	2.6	3	51	392	1,110
	5	32	3.5	10.7	217	3.1	3	54	325	690
Bronchi with	6	64	2.8	9.0	226	4.0	4	57	254	434
cartilage in wall	7	128	2.3	7.6	234	5.1	4	61	188	277
	8	256	1.86	6.4	240	7.0	4	66	144	164
	9	512	1.54	5.4	246	9.6	5	71	105	99
Terminal bronchus	10	1,020	1.30	4.6	250	13	6	77	73.6	60
	11	2,050	1.09	3.9	254	19	7	85	52.3	34
	12	4,100	0.95	3.3	257	29	10	95	34.4	20
Bronchioles with	13	8,190	0.82	2.7	260	44	12	106	23.1	11
muscle in wall	14	16,400	0.74	2.3	262	70	16	123	14.1	6.5
	15	32,800	0.66	2.0	264	113	22	145	8.92	3.6
Terminal bronchiole	16	65,500	0.60	1.65	266	180	30	175	5.40	2.0
Resp. bronchiole	17	131×10^3	0.54	1.41	267	300	42	217	3.33	1.1
Resp. bronchiole	18	262×10^3	0.50	1.17	269	534	61	278	1.94	0.57
Resp. bronchiole	19	524×10^3	0.47	0.99	270	944	93	370	1.10	0.31
Alveolar duct	20	1.05×10^6	0.45	0.83	271	1,600	139	510	0.60	0.17
Alveolar duct	21	2.10×10^6	0.43	0.70	271	3,200	224	734	0.32	0.08
Alveolar duct	22	4.19×10^6	0.41	0.59	272	5,900	350	1,085	0.18	0.04
Alveolar sac	23	8.39×10^6	0.41	0.50	273	12,000	591	1,675	0.09	—
Alveoli, 21 per duct		300×10^6	0.28	0.23	273		3,200	4,800		

[a]Area = total cross sectional area.
[b]Cum. = cumulative.
[c]Dead space, approx. 175 mL + 40 mL for mouth.

Source: Y.C. Fung (1990).

particles caused by the collision of gas molecules in air. The terminal settling velocity of a particle approaches 0.001 cm/s for a unit density sphere with a physical diameter of 0.5 μm, so that gravitational forces become negligible at smaller diameters. The main deposition mechanism is diffusion for a particle having physical (geometric) size <0.5 μm. Impaction and sedimentation are the main deposition mechanisms for a particle whose size is greater than 0.5 μm. Hence, d_{ae} = 0.5 μm is convenient for use as the boundary between the diffusion and aerodynamic regimes. Although this convention may lead to confusion in the case of very dense particles, most environmental aerosols have densities below 3 g/cm^3 (U.S. Environmental Protection Agency, 1982). Diffusional deposition is important in the small airways and in the A region where distances between the particles and airway epithelium are small. Diffusion has also been shown to be an important deposition mechanism in the ET region for small particles (Cheng et al., 1988, 1990).

With mouth-only breathing, the regional deposition pattern changes dramatically when compared to nasal breathing, with ET deposition being reduced and both TB and A deposition enhanced. Oronasal breathing (partly via the mouth and partly nasally), however, typically occurs in healthy adults while undergoing exercise. Therefore, the appropriate activity pattern of subjects for risk assessment estimation remains an important issue. Miller et al. (1988) examined ET and thoracic deposition as a function of particle size for ventilation rates ranging from normal respiration to heavy exercise. A family of estimated deposition curves was generated as a function of breathing pattern (See Section 10.5.1.4.). Anatomical and functional differences between adults and children are likely to interact with the major mechanisms affecting respiratory tract deposition in a complex way which will have important implications for risk assessment.

Humidification and warming of the inspired air begins in the nasal passages and continues into the deep lung. This conditioning of the ambient air does not significantly affect particle deposition unless the particulate material is intrinsically hygroscopic, in which case, it is very important. For both liquid and solid aerosol particles that are hygroscopic, there are physical laws that control both particle growth and deposition, and these have been modeled extensively. In a review of this general subject (Morrow, 1986), many experimental measurements of the humidity (RH) and temperature of the air within the respiratory tract have been reported, but because of the technical problems involved, uncertainties remain. Two major problems prevail:

(1) the accurate measurement of temperature requires a sensor with a very rapid response time; and (2) hygrometric measurements of conditions of near saturation (>99% RH) are the most difficult to make. The latter technicality is of special significance, because the growth of hygroscopic aerosols are greatest near saturation. For example, the effect of a difference in humidity between 99.0% and 99.9% is more important than the difference between 20 and 80% RH. A more complete discussion of models and experimental determinations of the deposition of hygroscopic aerosols is given in Section 10.4.

The differences in respiratory tract anatomy summarized briefly in this section are the structural basis for the species differences in particle deposition. In addition to the structure of the respiratory tract, the regional thickness and composition of the airway epithelium (a function of cell types and distributions) are important factors in clearance (Section 10.4). Characteristic values and ranges for many respiratory parameters have been published for "Reference Man" by the International Commission on Radiological Protection (ICRP) (1975) and they are also available from many reference sources (Altose, 1980; Collett et al., 1988; Cotes, 1979). A typical description of respiratory tract morphology, cytology, histology, structure, and function is given in Table 10-3. This description of the respiratory tract is used in the human dosimetry model applied in Section 10.7 (ICRP66, 1994). For additional information on human respiratory tract structure, the papers of Weibel (1963; 1980), Hatch and Gross (1964), Proctor (1977), Forrest (1993), and Gehr (1994) are recommended.